



Hydraulic Fluid Temperature -Imposed Nonlinearities in Automotive Active Hydraulic Suspension Systems

Received 30 July 2023; Revised 11 March 2024; Accepted 11 March 2024

¹Yousra A. Gazaz

²M-Emad S. Soliman

³Mahmoud Abdelrahim

⁴Aly S. Abo El-Lail

Keywords

ISO VG 22 fluid viscosity, Hydraulic actuator, Active Vehicle Suspension, Non-linear Model, Quarter Car Model, Nonlinear actuator dynamics, PID controller, Road Profile.

Abstract: In hydraulic active suspension systems, an often-overlooked source of nonlinearity is the performance deviation of the working hydraulic oil through the wide band of operating temperatures. In this paper, a quarter-car, Simulink® Simscape nonlinear hydraulic active suspension model has been constructed, taking ISO VG 22 oil as the working oil[1]. A PID controller has been tuned for the active suspension system. Targeted response parameters were tire deflection and suspension travel, as measures of vehicle handling, and sprung-mass acceleration as a measure of riding comfort. At a typical moderate vehicle speed of 40 km/hr, system response was investigated for both single sinusoidal bump and continuous wavy sinusoidal road inputs. Simulation was performed at two distant, extreme, operating temperatures, namely 60°C and -30°C. Results showed that at higher temperatures, the decrease in oil viscosity of the hydraulic actuator results in higher tire-rebound amplitudes and longer settling times, and a higher sprung mass acceleration amplitude, worsening both tire-road holding, and ride comfort compared to those at -30°C. The most significant conclusion is that an active suspension's hydraulic actuator actually behaves as a nonlinear damper, besides being a force generator.

1. Introduction

Vehicle suspension connects vehicle wheels to vehicle body via springs, dampers, and associated linkages. Springs support vehicle body weight, absorb and store energy, thus isolate vehicle body from road disturbances. Dampers, on the other hand, dissipate this stored energy and thus damp potential oscillations[2],[3]. A suspension system supports

¹Instructor at Egyptian German College of Technology, MITU University. yousragazaz@gmail.com

²Emeritus Professor, Mechanical Engineering Design and Production Dept., Assiut University, Egypt. Emadd9991@gmail.com

³Assoc. Professor at the Department of Mechatronics Engineering, Assiut University, Assiut, Egypt. m.abdelrahim@aun.edu.eg

⁴Dept. of Mechanical Engineering, Faculty of Engineering, Assiut University, Assiut, Egypt. ali.abouelail@eng.au.edu.eg

both the static and dynamic weight of a vehicle. This task is bounded by the suspension rattle space and depends on the suspension type used[4].

One major objective of a vehicle's suspension is to provide robust vehicle handling and road holding against road roughness, irregularities, and disturbances (bumps and potholes), and to maintain stability, safety, and control during critical maneuvers, such as acceleration, braking, cornering, and lane changes[5],[6]. It is not simple to quantify vehicle handling and road holding issues due to their subjective nature. However, tire deflection is commonly used as a simple, measurable road holding index as changes in normal tire forces are sensed through variation in tire deflection[7],[8]. A zero or negative tire-deflection warns against tire-road separation. Besides, a non-positive suspension-travel value occurs when wheel assembly is freely suspended, an indication of vehicle jumps and consequent tire-road separation.

The second major aim of a suspension is to provide good ride comfort, which, in turn, is another subjective issue. However, many experimental studies have proven that ride comfort is correlated with the vertical acceleration level in the low-frequency range of 1 to 1.5 Hz[9],[10],[11]. For passive suspension, ride comfort and road holding are two conflicting aspects that are simply correlated to the stiffness of the suspension. A softer suspension ensures ride comfort at the expense of degraded road holding and vice versa.

By regulating tire/road adhesion forces, active vehicle suspensions, on the other hand, provide both increased road holding safety and ride comfort by eliminating road irregularities[12],[13].

Vehicle suspensions, even passive ones, are inherently non-linear. Typical embedded passive suspension nonlinearities are associated with hardening springs, quadratic dampers, and/or the tire/road separation phenomenon. Active Suspensions, on the other hand, add numerous nonlinearities associated with and correlated to the type and design of the actuation system. Consequently, in real vehicles, it is ultimately hard to achieve desired performance via application of linear control techniques. In hydraulic active suspension systems, a source of nonlinearity, that is often overlooked, may be allocated to performance deviations of the working hydraulic oil caused by the wide band of operating temperatures. Electro-hydraulic actuators are commonly applied to generate vibration isolation forces in active suspensions[14], [15]. The active force is modulated via the voltage applied to the hydraulic actuator[16]. This voltage is correlated to hydraulic oil density, oil supply pressure, piston effective area, hydraulic- cylinder leakage coefficient, and oil's elastic stiffness.

It is important to note that, in many literatures, actuators are modeled as ideal force generators, which is not practical[17]. Electro-hydraulic actuators are inherently highly nonlinear. To avoid performance deviations, dynamic characteristics of actuators should be considered. Recently, compensation for nonlinearities in electro-hydraulic actuators of active vehicle suspensions have been extensively researched[18], [19] and[20] . SU[21] proposed a master-slave control law to solve the input nonlinearity of the hydraulic active

suspension system. A robust H_∞ control was implemented to deal with the problems of input delay, parameter uncertainties, and multi-objective optimization in the linear system. Yao et al[22] proposed a desired- compensation adaptive controller for high-precision motion control of electro-hydraulic servo systems, considering nonlinearity, modeling uncertainties, and severe measurement noise arising from actual-state feedback. PID controllers for active suspensions are designed by tuning for improving handling and riding comfort[23], [24]. Dangor et al[25] designed a PID controller for an electrohydraulic active suspension system using evolutionary algorithms (EA), definitely, particle swarm optimization (PSO), genetic algorithm (GA), and differential evolution (DE). All these algorithms showed overall improvement in suspension travel, ride comfort, settling time, and road holding. However, these improvements were at the cost of increased actuator force, power consumption, and spool-valve displacement.

In the previously mentioned literature, however, uncertainties due to changes in physical characteristics in the actuator system have not been considered. For instance, the hydraulic oil temperature varies continuously during vehicle operation. Consequently, uncertainties in the density and viscosity of hydraulic oil arise. To solve this problem, continuous adaptive changes in physical characteristics of the hydraulic actuator should be considered. The objective of the present study is to simultaneously optimize ride comfort and road holding performances considering hydraulic fluid performance temperature variations. PID control has been applied for optimal control. A non-linear model of a hydraulic active suspension system is used to explore nonlinearities caused by temperature changes of hydraulic oil. Simulation of both handling and ride performances for the hydraulic active suspension at typical extreme working temperatures is presented. Simulation is carried out using SIMULINK's Simscape library.

2. System Modeling

2.1. Quarter Car Model

A quarter-car model of the active suspension system is shown in Figure-1. The model is composed of two lumped masses modeling the vehicle body as a sprung mass, M_s and the wheel assembly as an unsprung mass, M_u . Active suspension parameters are the spring stiffness, K_s , damping coefficient C_s and hydraulic actuator force, F_a . Tire elastic and damping properties are modeled as K_t and C_t respectively. Road profile input to the model is represented by x_r . Both tire deflection ($x_t = x_r - x_u$) and suspension travel ($x_p = x_s - x_u$) are measured and compared to reference set points. The required actuator force, F_a is to be determined by the controller to eliminate the error. Dynamic equations of the quarter- car active suspension system are given as:

$$M_s \ddot{x}_s + C_s (\dot{x}_s - \dot{x}_u) + K_s (x_s - x_u) = F_a \quad \text{Eq. (1)}$$

$$M_u \ddot{x}_u + C_s (\dot{x}_u - \dot{x}_s) + C_t (\dot{x}_u - \dot{x}_r) + K_s (x_u - x_s) + K_t (x_u - x_r) = - F_a \tag{Eq. (2)}$$

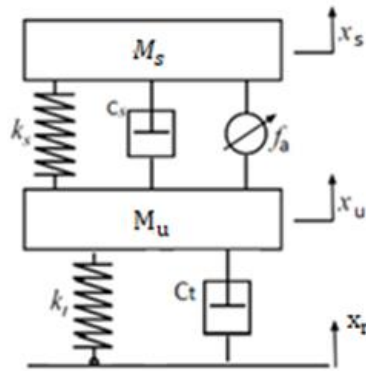


Fig.1: Quarter-car vehicle model with active hydraulic actuation.

2.2. Electro-Hydraulic Active Actuator Model ([26], [27], [18] and[29])

The main components of a hydraulic active suspension system are typically a hydraulic actuator, a hydraulic pump, a servo valve, and an oil reservoir.

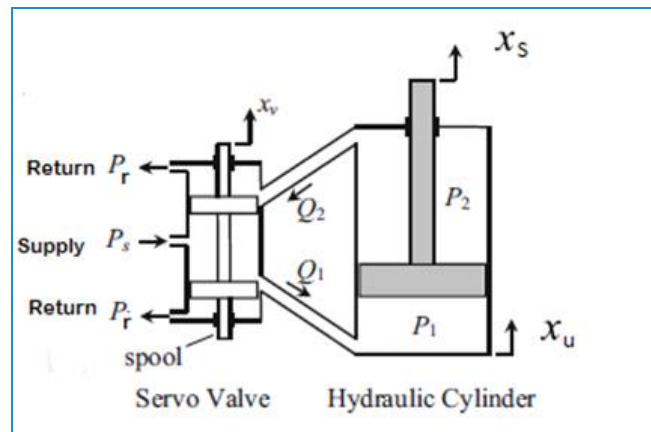


Fig.2: Hydraulic servo system

The hydraulic actuation force is given by:

$$F_a = A_p \cdot p_L \tag{Eq. (3)}$$

Where A_p is the piston area and p_L is the net pressure difference between piston faces,

$$p_L = p_1 - p_2 \tag{Eq. (4)}$$

In this design a three-land, 4-way spool valve is assumed, therefore,

$$\dot{p}_L = -\beta p_L - \sigma A_p (\dot{x}_s - \dot{x}_u) + \gamma x_v \sqrt{(p_s - p_L \operatorname{sgn} x_v)} \tag{Eq. (5)}$$

Where: $\beta = \sigma.C_{tp}$, $\gamma = \sigma.C_d.W.S\sqrt{\frac{1}{\rho}}$, $\sigma = \frac{4\beta_e}{V_t}$

The parameters β_e , V_T , C_{tp} , C_d , ρ , W , S , and p_s , are defined and their values given in table (1). In electrohydraulic actuation, servo valve displacement and velocity (x_v and \dot{x}_v) are controlled via an input voltage signal, u_m , according to:

$$\dot{x}_v = \frac{1}{\tau}(u_m - x_v) \tag{Eq. (6)}$$

Now, to get the state-space form, let's define:

$$\begin{aligned} x_1 &= x_s - x_u & x_2 &= \dot{x}_s & x_3 &= x_u - x_r \\ x_4 &= \dot{x}_u & x_5 &= p_L & x_6 &= x_v \end{aligned}$$

The state-space representation of equations (1 and 2) becomes:

$$\dot{x}_1 = x_2 - x_4 \tag{Eq. (7)}$$

$$\dot{x}_2 = -\frac{K_s}{M_s}x_1 - \frac{C_s}{M_s}x_2 + \frac{C_s}{M_s}x_4 - \frac{A_p}{M_s}x_5 \tag{Eq. (8)}$$

$$\dot{x}_3 = x_4 - \dot{x}_r \tag{Eq. (9)}$$

$$\dot{x}_4 = -\frac{K_t}{M_u}x_3 - \frac{C_t}{M_u}x_4 + \frac{K_s}{M_u}x_1 - \frac{C_s}{M_u}x_2 - \frac{C_s}{M_u}x_4 - \frac{A_p}{M_u}x_5 \tag{Eq. (10)}$$

$$\dot{x}_5 = -\beta x_5 - \sigma A_p x_2 + \sigma A_p x_4 + \gamma x_6 \sqrt{p_s - x_5} \operatorname{sgn} x_6 \tag{Eq. (11)}$$

$$\dot{x}_6 = \frac{1}{\tau}(u_m - x_6) \tag{Eq. (12)}$$

Where sgn stands for the sign of the variable following it.

Table 1. Hydraulic active suspension system parameters.

Parameter		Units	Value	Parameter		Units	Value
M_s	Sprung mass (Vehicle chassis mass)	kg	300	M_u	Unsprung mass (Wheel-assembly mass)	kg	60
K_s	Suspension Spring Stiffness	kN/m	16	K_t	Equivalent Tire Stiffness	kN/m	190
C_s	Suspension Damping coefficient.	Ns/m	1000	C_t	Equivalent Tire damping coefficient	Ns/m	800
A_p	Effective cross-sectional area of piston	m^2	3.35×10^{-4}	C_d	Discharge coefficient	--	0.63

Parameter		Units	Value	Parameter		Units	Value
β_e	Effective elastic modulus of Oil	MPa	900	ρ	Fluid density	kg/m ³	870
V_t	volume	m ³	3.12 x10 ⁻⁴	P_s	Supply pressure	kPa	20 x10 ³
C_{tp}	Piston leakage coefficient	m ⁵ /(N.s)	9.047 x 10 ⁻¹³	P_l	Load pressure	kPa	16 x10 ³
σ	A hydraulic coefficient	N/m ⁵	2.273 x10 ⁹	W	Spool valve width	m	0.008
F_a	control force	N		η	Area ratio	--	0.685
x_v	Servo-valve displacement	mm		u_m	voltage input signal	v	
				\dot{x}_v	Servo-valve velocity	mm/s	

3. Controller Design

3.1. Control Objectives

The active control targets the following:

1. Keeping a minimal positive tire deflection, to assure good grip and no tire separation.
2. Minimum suspension travel, as a measure of good handling.
3. Minimum body acceleration, as an index for passenger comfort.
4. Reasonable control bandwidth: (high speed of response)

3.2. Control architecture.

Vehicle model has only two inputs, namely, the road disturbance, x_r and the actuator force, F_a . Model outputs are tire deflection, suspension travel, sprung-mass displacement, and acceleration. Actuator control signal is estimated based on the continuously measured inputs. PID control is the most popular type of feedback control. Its well-known controller equation is:

$$u(t) = k_p \cdot e(t) + k_i \cdot \int e(t) \cdot dt + k_d \cdot \frac{d}{dt} e(t) \tag{Eq. (13)}$$

Where $u(t)$ is the system's control signal, $y(t)$ is the actual output, and $r(t)$ is the desired reference output (set point). $e(t)$ Is the continuously monitored error: $e(t) = r(t) - y(t)$. Desired closed-loop dynamics are obtained by adjusting the three control parameters K_P , K_i , and K_D , often iteratively via "tuning" and without specific knowledge of a plant's model. The proportional term always correlates to stability, the integral term permits the rejection of a step disturbance, while the derivative term provides damping or shaping of the response. The Simscape model of the active suspension system using a PID controller is given in Fig. 3.

4. Simulation of System Response:

Based on a quarter-car model, a simulation model focusing on tire-road holding and ride comfort was built using MATLAB®'s SIMSCAPE® simulation software, where road disturbance is assumed as the input for the system. Targeted response parameters are tire deflection, suspension travel, sprung-mass acceleration, and displacement. The control objective is to prevent tire-road separation while maintaining reasonable suspension travel, and, at the same time, minimize sprung-mass acceleration. Active suspension response results for two different inputs, namely; a single sinusoidal road bump and a wavy sinusoidal road are presented.

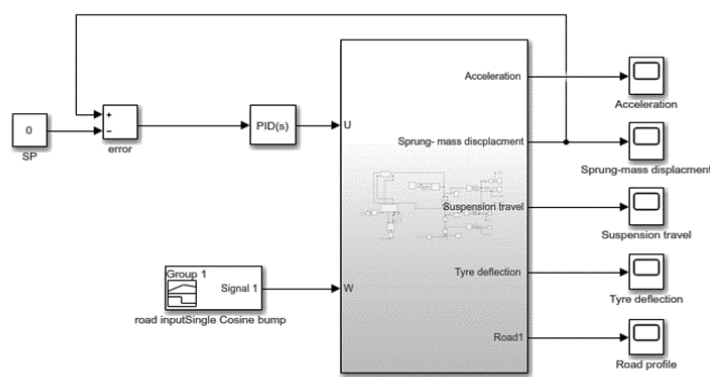


Fig.3: Simulink's Simscape model of the active suspension system using a PID Controller.

5.1 Effect of Oil's Operating Temperatures on the Hydraulic Active System Response:

5.1.1 Response to a Sinusoidal Road Bump:

To reveal the nonlinear behavior of oil in the hydraulic actuator, system response to a 100 mm peak single sinusoidal bump at two distant, extreme, operating temperatures, namely -30°C and 60°C was investigated at a moderate vehicle speed of 11.11 m/s (40 km/hr). Simulation was performed taking ISO VG 22 oil as the working hydraulic oil[1]. Simulation results are presented in figures 4 through 13 below.

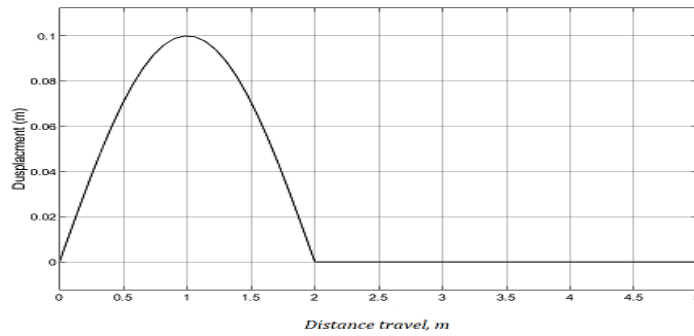


Fig.4: A sinusoidal bump road profile with a 0.1 m amplitude.

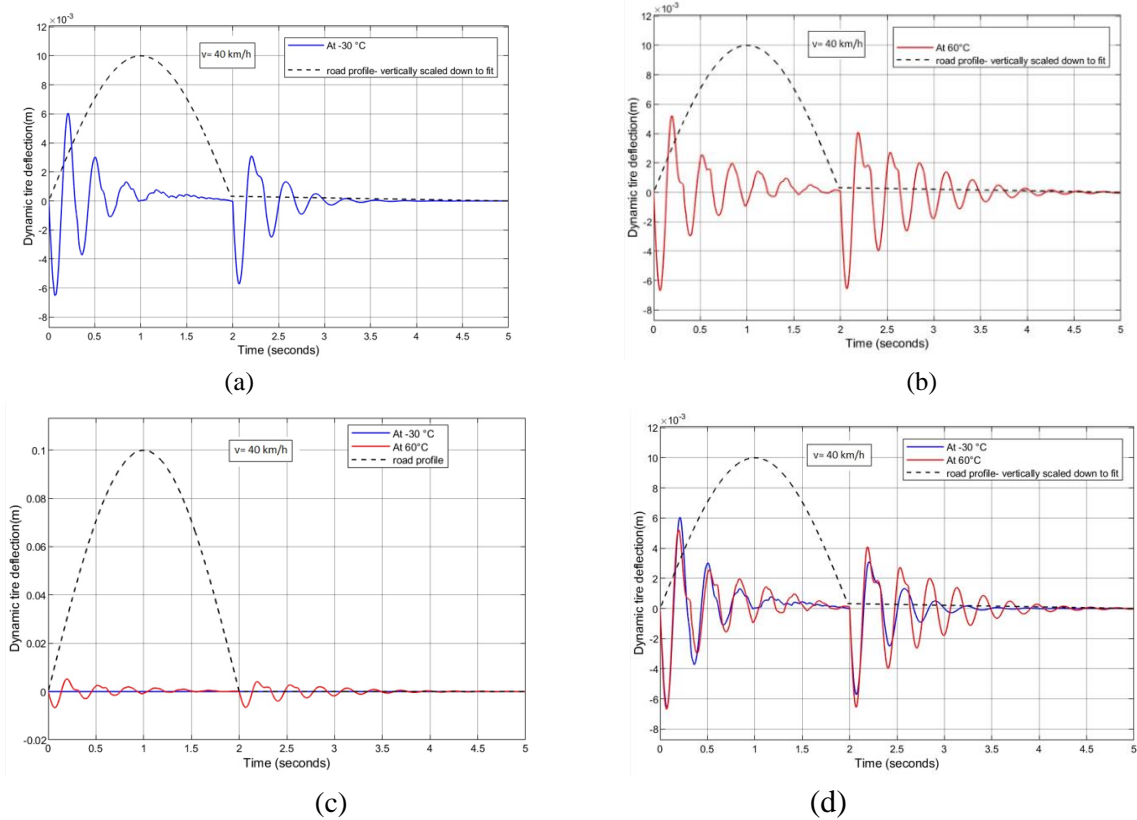


Fig. 5: Dynamic tire deflection response to a sinusoidal road bump at a speed of 40 km/h for different operating temperatures:

- (a) At -30 ° C.
- (b) At 60 ° C.
- (c) Superimposed plots for relative comparison.
- (d) Relative to bump size.

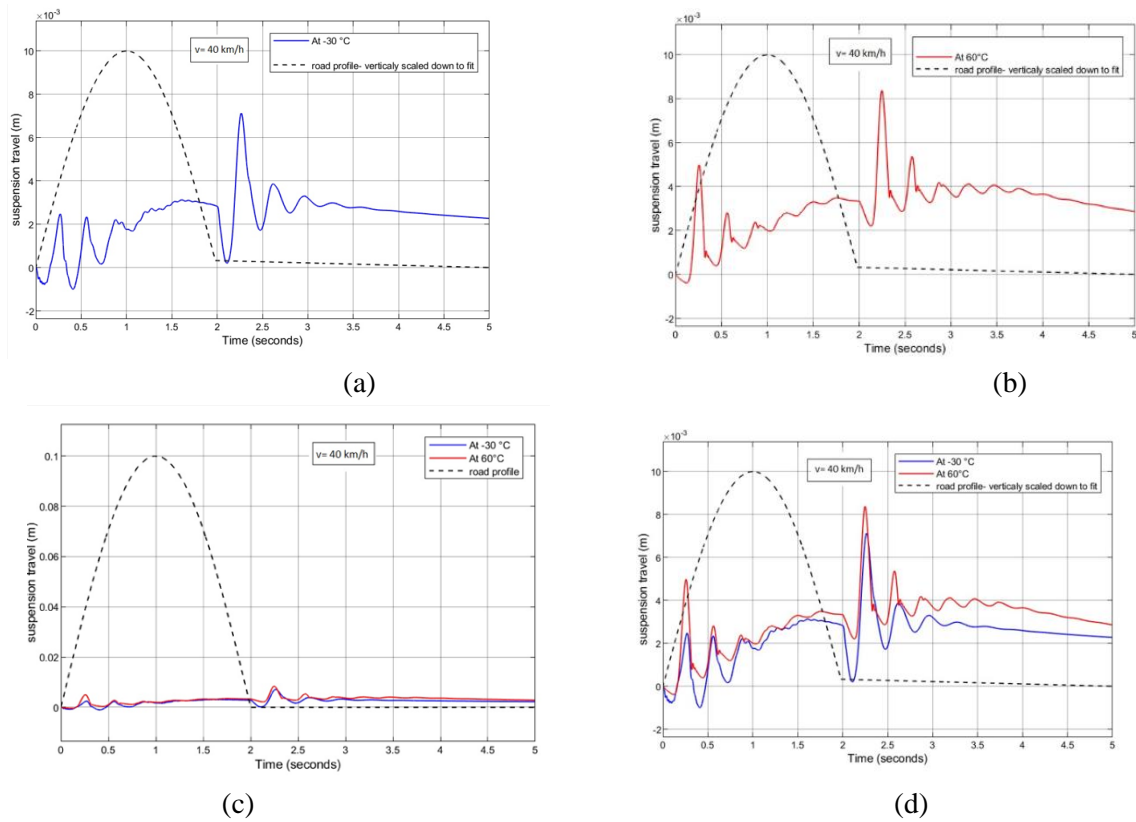


Fig. 6: Suspension travel response to a sinusoidal road bump at a speed of 40 km/h for different operating temperatures:

- (a) At -30 °C
- (b) At 60 °C
- (c) Superimposed plots for relative comparison
- (d) Relative to bump size.

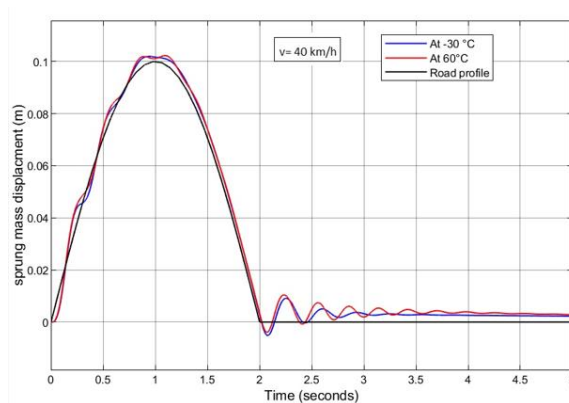


Fig. 7: Sprung-mass displacement response to a sinusoidal bump at a speed of 40 km/h for different operating temperatures.

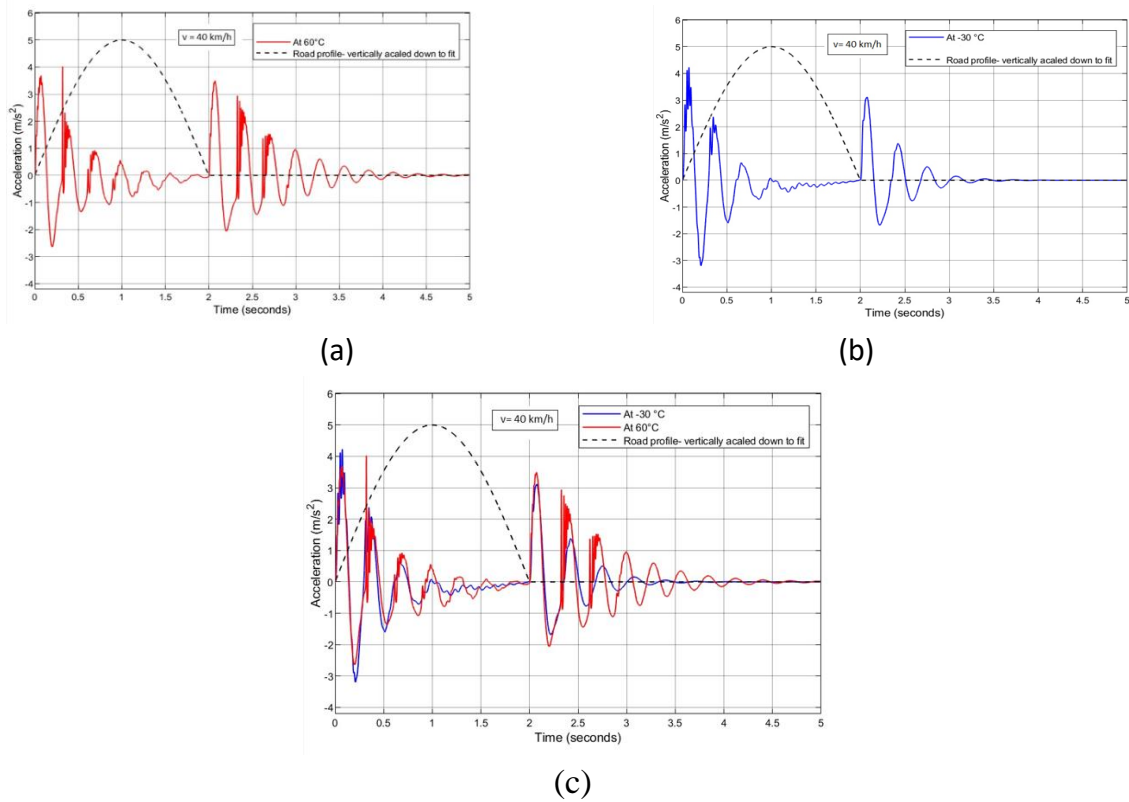


Fig. 8: Sprung-mass acceleration response to a sinusoidal road bump at a speed of 40 km/h for different operation temperatures:

- (a) At $-30\text{ }^{\circ}\text{C}$
- (b) At $60\text{ }^{\circ}\text{C}$
- (c) Cumulative curve for relative comparison

5.1.2. System Response to a Wavy Sinusoidal Road.

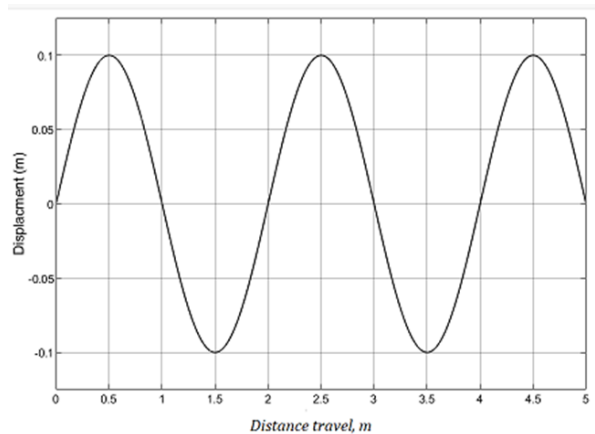


Fig. 9: A continuous sine wave road profile with amplitude of 0.1 m

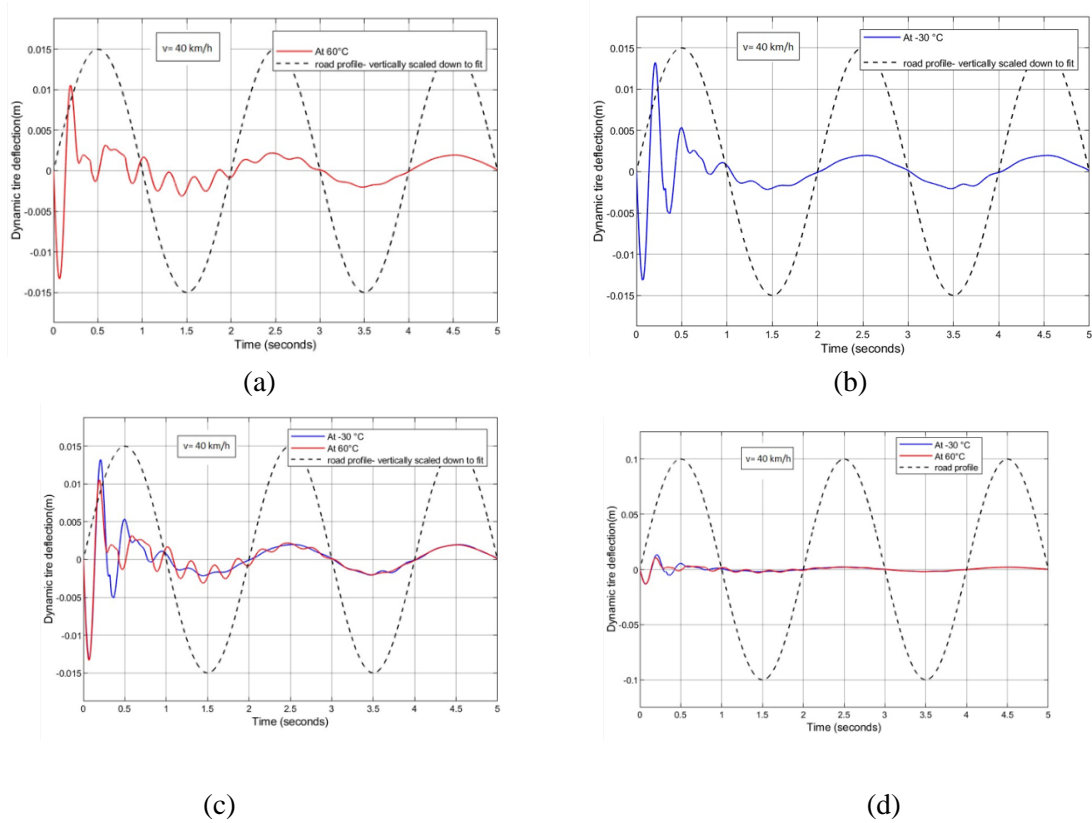


Fig. 10: Dynamic tire deflection response to a wavy sinusoidal road at a speed of 40 km/h for different operating temperatures:

- (a) At -30 °C
- (b) At 60 °C
- (c) Cumulative curve for relative comparison.
- (d) Relative to bump size.

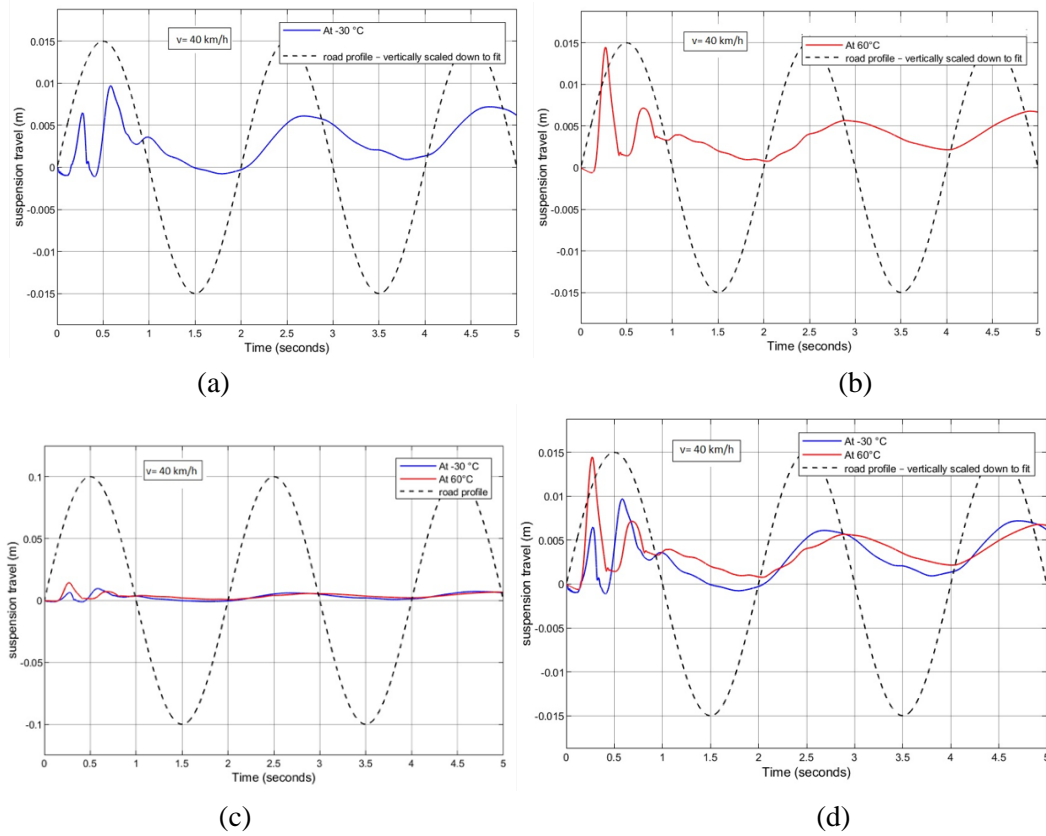


Fig. 11: Suspension travel response to a wavy sinusoidal road at a speed of 40 km/h for different operating temperatures:

- (a) At -30 °C
- (b) At 60 °C
- (c) Cumulative curve for relative comparison.
- (d) Relative to bump size.

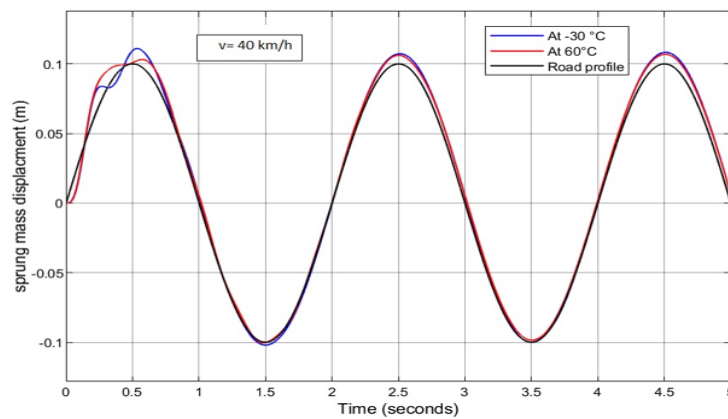


Fig 12: Sprung-mass displacement response to a wavy sinusoidal road at a speed of 40 km/h for different operating temperatures.

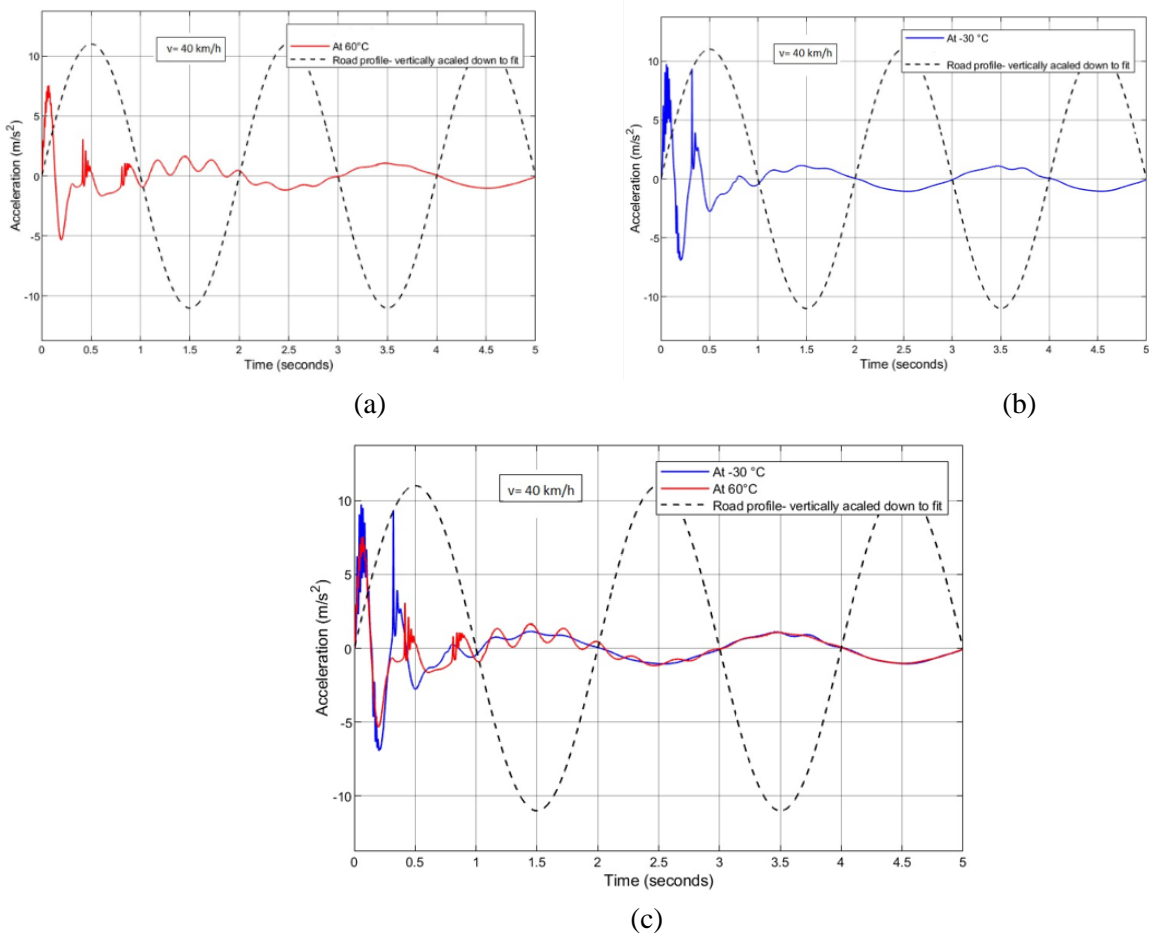


Fig. 13: Sprung-mass acceleration response to a wavy sinusoidal road at a speed of 40 km/h for different operating temperatures:

- (a) At -30 ° C
- (b) At 60 ° C
- (c) Cumulative curve for relative comparison.

6 Results

Table: 2. RMS response values to a Sinusoidal Bump input at temperatures of -30° C and 60° C.

No.	Parameter RMS	at -30° C	at 60° C	Percentage Change
1	Sprung mass acceleration, m/s ²	0.9907	1.016	2.55
2	Suspension deflection, m	2.32×10 ⁻³	2.8×10 ⁻³	20.326
3	Sprung-mass displacement, m	6.14×10 ⁻²	6.209×10 ⁻²	1.087

Table: 3. RMS response values to a wavy sinusoidal road input at temperatures of- 30° C and 60° C.

No.	Parameter RMS	at -30° C	at 60° C	Percentage Change
1	Sprung mass acceleration, m/s^2	2.021	1.685	-19.94
2	Suspension deflection, m	3.44×10^{-3}	4.638×10^{-3}	36.13
3	Sprung-mass displacement, m	7.716×10^{-2}	7.778×10^{-2}	0.80

7 Discussion/Conclusion

A quarter-car, Simulink® Simscape nonlinear hydraulic active suspension model has been constructed utilizing data extracted from [28]. Dynamics of the hydraulic actuator have been included in the model. A PID controller has been tuned for the active suspension system. System response was investigated for both a single sinusoidal bump and a continuous wavy sinusoidal road input, both having a 100 mm amplitude.

7.1 A Sine Road Bump:

Regarding road holding and vehicle handling, figure (5) reflects the nonlinear behavior of the hydraulic actuator due to viscosity-temperature changes. At higher temperatures, the decrease in viscosity results in a higher tire-rebound frequency, thus worsening tire-road holding and vehicle handling. Moreover, there is a noticeable increase in the after-bump tire bouncing amplitudes and the settling time for tire oscillation is doubled to 60°C compared to that at -30°C. This reflects the fact that a hydraulic actuator actually behaves as a nonlinear damper, besides being a force generator. In both cases, however, tire deflection did not exceed a maximum of 6% of the bump height.

On the other hand, suspension travel curve, figure (6) shows that at higher temperatures suspension acquires a highly- increased travel amplitude during the “uphill” stage and after the end of the “downhill” stage of that bump. Throughout the entire response cycle, suspension travel attains higher values than at cold temperatures. The peak travel values are 8% and 7% of the bump height at 60°C and -30°C respectively. However, the negative part of the curve is eliminated at higher temperatures. This fortunately indicates better road holding and vehicle handling stability.

Regarding passenger comfort, at higher temperatures, acceleration amplitudes are greater during the “after- bump” stage, and takes longer time to sustain, worsening the vehicle-ride comfort. Simulation results also show that at freezing (-30°C) the maximum peak of sprung mass displacement response reached 8 mm while at a high temperature (60°C) the same peak exceeds 10 mm. Moreover, at higher temperatures, the “after-bump “sprung mass oscillations take longer time to sustain. This is due to changes in both viscosity and the bulk modulus of hydraulic actuator oil.

7.2 A sinusoidal wavy road:

For a sinusoidal wavy road, system response is similar in the first sine bump of the road but sustained thereafter. After the first cycle of the continuous “sine bump”, tire deflection appears to smoothly adapt to the road waves with almost zero-amplitude higher harmonic oscillations. It appears to acquire a smooth deflection in phase with road texture and with an amplitude which is almost 2% of the road’s sine amplitude.

Suspension travel follows a rectified sine shape after the first road wave cycle, with almost zero negative travel at both higher and lower temperatures, reflecting a better road holding. Sprung mass displacement closely coincides with road amplitude after the first road cycle, with slightly higher amplitude at the higher temperature. However, sprung mass acceleration looks smooth with low amplitude value and no harmonics after the first road cycle, meaning an improved ride comfort with no significant discrepancy between the higher and lower temperatures.

Generally, it could be said that the viscosity-caused non-linearity is noticeable only in the first sine bump which represents half of the first road cycle.

References

- [1] A. Pcr and L. Kit, “Data Sheet Data Sheet,” *고생물학회지*, vol. 31402, no. September 2004, pp. 0–1, 2012, [Online]. Available: http://www.papersearch.net/view/detail.asp?detail_key=10000715.
- [2] K. Efatpenah, J. H. Beno, and S. P. Nichols, “Energy requirements of a passive and an electromechanical active suspension system,” *Veh. Syst. Dyn.*, vol. 34, no. 6, pp. 437–458, 2000, doi: 10.1076/vesd.34.6.437.2050.
- [3] P. A. Yadav, “Suspension System with its Different Models and Classifications,” vol. 10, no. 61, pp. 10–15, 2015.
- [4] C. Kim and P. I. Ro, “A sliding mode controller for vehicle active suspension systems with non-linearities,” *Proc. Inst. Mech. Eng. Part D J. Automob. Eng.*, vol. 212, no. 2, pp. 79–91, 1998, doi: 10.1243/0954407981525812.
- [5] M. S. Kumar and S. Vijayarangan, “Analytical and experimental studies on active suspension system of light passenger vehicle to improve ride comfort,” *Mechanika*, vol. 65, no. 3, pp. 34–41, 2007, doi: 10.5755/j01.mech.65.3.14828.
- [6] M. Senthil, “Development of Active Suspension System for Automobiles using PID Controller,” *Lect. Notes Eng. Comput. Sci.*, vol. II, 2008.
- [7] A. M. Al Aela, J. P. Kenne, and H. A. Mintsa, “A novel adaptive and nonlinear electrohydraulic active suspension control system with zero dynamic tire liftoff,” *Machines*, vol. 8, no. 3, 2020, doi: 10.3390/MACHINES8030038.
- [8] W. Sun, Y. Zhao, J. Li, L. Zhang, and H. Gao, “Active suspension control with frequency band constraints and actuator input delay,” *IEEE Trans. Ind. Electron.*, vol. 59, no. 1, pp. 530–537, 2012, doi: 10.1109/TIE.2011.2134057.
- [9] P. W. Johnson, “7th ACHV Proceeding bookpdf,” *Ind. Heal. Saf. Instrumentation*, 2018.
- [10] M. L. De la Hoz-Torres, A. J. Aguilar-Aguilera, M. D. Martínez-Aires, and D. P. Ruiz,

- “Assessment of whole-body vibration exposure using ISO2631-1:2008 and ISO2631-5:2018 standards,” *INTER-NOISE 2019 MADRID - 48th Int. Congr. Exhib. Noise Control Eng.*, 2019.
- [11] S. Mouleeswaran, “Design and Development of PID Controller-Based Active Suspension System for Automobiles,” *PID Controll. Des. Approaches - Theory, Tuning Appl. to Front. Areas*, 2012, doi: 10.5772/32611.
- [12] A. Agharkakli, G. S. Sabet, and A. Barouz, “Simulation and Analysis of Passive and Active Suspension System Using Quarter Car Model for Different Road Profile,” *Int. J. Eng. Trends Technol.*, vol. 3, no. 5, pp. 636–644, 2012.
- [13] J. Bharali and N. Garg, “Efficient Ride Quality and Road Holding Improvement for Active Suspension System,” *2017 14th IEEE India Counc. Int. Conf. INDICON 2017*, 2018, doi: 10.1109/INDICON.2017.8487904.
- [14] X. Shen and H. Peng, “Analysis of active suspension systems with hydraulic actuators,” *Veh. Syst. Dyn.*, vol. 41, no. SUPPL., pp. 143–152, 2004.
- [15] Y. M. Sam and K. Hudha, “Modelling and force tracking control of hydraulic actuator for an active suspension system,” *2006 1st IEEE Conf. Ind. Electron. Appl.*, 2006, doi: 10.1109/ICIEA.2006.257242.
- [16] S. Kilicaslan, “Control of active suspension system considering nonlinear actuator dynamics,” *Nonlinear Dyn.*, vol. 91, no. 2, pp. 1383–1394, 2018, doi: 10.1007/s11071-017-3951-x.
- [17] E. Mahmoud, M. Atef, and A.-E. Hameed, “Automatic control of vehicle active suspension systems.”
- [18] Y. Huang, J. Na, X. Wu, and G. Gao, “Approximation-Free Control for Vehicle Active Suspensions with Hydraulic Actuator,” *IEEE Trans. Ind. Electron.*, vol. 65, no. 9, pp. 7258–7267, 2018, doi: 10.1109/TIE.2018.2798564.
- [19] E. S. Kim, “Nonlinear indirect adaptive control of a quarter car active suspension,” *IEEE Conf. Control Appl. - Proc.*, pp. 61–66, 1996, doi: 10.1109/cca.1996.558605.
- [20] F. Ding, X. Han, C. Jiang, J. Liu, and C. Peng, “Fuzzy Dynamic Output Feedback Force Security Control for Hysteretic Leaf Spring Hydro-Suspension With Servo Valve Opening Predictive Management Under Deception Attack,” *IEEE Trans. Fuzzy Syst.*, vol. 30, no. 9, pp. 3736–3747, 2022, doi: 10.1109/TFUZZ.2021.3128056.
- [21] X. Su, “Master-slave control for active suspension systems with hydraulic actuator dynamics,” *IEEE Access*, vol. 5, no. c, pp. 3612–3621, 2017, doi: 10.1109/ACCESS.2017.2672598.
- [22] J. Yao, W. Deng, and W. Sun, “Precision Motion Control for Electro-Hydraulic Servo Systems with Noise Alleviation: A Desired Compensation Adaptive Approach,” *IEEE/ASME Trans. Mechatronics*, vol. 22, no. 4, pp. 1859–1868, 2017, doi: 10.1109/TMECH.2017.2688353.
- [23] M. Avesh and R. Srivastava, “Modeling simulation and control of active suspension system in Matlab Simulink environment,” *2012 Students Conf. Eng. Syst. SCES 2012*, pp. 0–5, 2012, doi: 10.1109/SCES.2012.6199124.
- [24] K. D. Rao, “Modeling, simulation and control of semi active suspension system for automobiles under MATLAB Simulink using PID controller,” *IFAC Proc. Vol.*, vol. 3, no. PART 1, pp. 827–831, 2014, doi: 10.3182/20140313-3-IN-3024.00094.

-
- [25] M. Dangor, O. A. Dahunsi, J. O. Pedro, and M. M. Ali, "Evolutionary algorithm-based PID controller tuning for nonlinear quarter-car electrohydraulic vehicle suspensions," *Nonlinear Dyn.*, vol. 78, no. 4, pp. 2795–2810, 2014, doi: 10.1007/s11071-014-1626-4.
- [26] C.-M. Ong, *Modeling of Dynamic Systems*, vol. 5. 1998.
- [27] Ramin S. Esfandiari Bei Lu, *Modeling and Analysis of DYNAMIC SYSTEMS*, SECOND Edi. 2002.
- [28] F. Ding, H. Shan, X. Han, C. Jiang, C. Peng, and J. Liu, "Security-Based Resilient Triggered Output Feedback Lane Keeping Control for Human–Machine Cooperative Steering Intelligent Heavy Truck Under Denial-of-Service Attacks," *IEEE Trans. Fuzzy Syst.*, vol. 31, no. 7, pp. 2264–2276, 2023, doi: 10.1109/TFUZZ.2022.3222905.
- [29] M. A. Nekoui and P. Hadavi, "Optimal control of an active suspension system," *Proc. EPE-PEMC 2010 - 14th Int. Power Electron. Motion Control Conf.*, pp. 60–63, 2010, doi: 10.1109/EPEPEMC.2010.5606776.
- [30] J. K. Hedrick and M. D. Donahue, "Implementation of an Active Suspension," *Nonlinear Hybrid Syst. Automot. Control*, vol. XVIII, p. 446, 2003.
- [31] R. B. M. and S. D. F. J.A.LEVITT, "Non-linear dynamic modeling of an automobile hydraulic active suspension system," *Mech. Syst. Signal Process.*, vol. 8, no. 5, pp. 485–517, 1994, doi: 10.1006.

السلوك اللاخطي الناتج عن تغير درجة حرارة السائل في الانظمة الهيدروليكية للتعليق النشط

الملخص:

في أنظمة التعليق النشطة الهيدروليكية، يُعتبر تحول أداء زيت التشغيل الهيدروليكي عبر النطاق الواسع لدرجات الحرارة التشغيلية من مصادر عدم اللاخطية التي غالبًا ما يتم تجاهلها في هذا البحث، تم إنشاء نموذج هيدروليكي ربع سيارة غير خطي باستخدام برنامج Simulink® Simscape ، مع استخدام زيت ISO VG 22 كزيت تشغيل [1]. تم ضبط وحدة التحكم PID لنظام التعليق النشط. كانت معلمات الاستجابة المستهدفة هي انحراف الإطار وحركة التعليق، كمقاييس للتعامل مع السيارة، وتسارع الكتلة السيارة كمقياس لراحة الركوب. تمت دراسة استجابة النظام لكل من مدخلات الطريق الجيبية المفردة ومدخلات الطريق الجيبية المتموجة المستمرة عند سرعة متوسطة تبلغ ٤٠ كم/ساعة. تم إجراء المحاكاة عند درجتي حرارة تشغيليتين متباعدتين، وهما ٦٠ درجة مئوية و-٣٠ درجة مئوية. أظهرت النتائج أنه عند درجات الحرارة المرتفعة، يؤدي انخفاض لزوجة الزيت في المحرك الهيدروليكي إلى زيادة سعة ارتداد الإطار، وزيادة سعة تسارع الكتلة السيارة المعلقة ، مما يؤدي إلى تفاقم ثبات الإطار على الطريق وراحة الركوب مقارنة بتلك الموجودة في -٣٠ درجة مئوية. الاستنتاج الأكثر أهمية هو أن المحرك الهيدروليكي لنظام التعليق النشط يتصرف في الواقع كمخمد غير خطي، إلى جانب كونه مولدًا للقوة.